EuroGeo4 paper number 285

EVALUATION OF STEPPED ISOTHERMAL METHOD USING TWO TYPES OF GEOGRIDS

Sang-Sik Yeo[1] & Y. Grace Hsuan[2]

[1] *Geosyntec Consultants, San Diego, CA 92127, USA (e-mail: syeo@geosyntec.com)*
[2] *Department of Civil, Architectural and Environmental Engineering, Drexel University, Philadelphia, PA 19104, USA (e-mail: ghsuan@coe.drexel.edu)*

Abstract: The Stepped Isothermal Method (SIM) designated as ASTM D 6992-03 was evaluated using polyester (PET) and high density polyethylene (HDPE) geogrids. SIM has been a well accepted creep acceleration method to assess the creep behavior of PET geogrids while it has not been thoroughly studied for HDPE geogrids. In this paper, the non-equilibrium stage at the beginning of each elevated temperature step was found in both geogrids; particularly the HDPE geogrid. The non-equilibrium stage was caused by a thermal expansion under the immediate temperature increase. A modified SIM (MSIM) was introduced by removing the non-equilibrium stage of the creep curve at each elevated temperature in the analysis of the SIM test data. The creep master curves from MSIM and SIM were compared to that of Time-Temperature Superposition (TTS). For the PET geogrid, three master curves were very similar; however, the similarity of three curves was limited to the linear creep curve at strain below 10% for the HDPE geogrid. For the non-linear portion of the creep curves, SIM was found underestimating the creep deformation in comparison to MSIM and TTS. In addition to the comparison of creep curves, similar activation energy values were obtained for the PET geogrid regardless the method, while variation was found for the HDPE geogrid.

Keywords: creep, high density polyethylene (HDPE), polyester, stepped isothermal method,

INTRODUCTION

Geogrids are widely used in walls, slopes, foundations, and roads as reinforcement in which they are subjected to constant stress throughout their service life (Carroll and Chouery-Curtis 1991; Koerner 2005; Fannin 2001). Many design methods utilize long-term strength that incorporates reduction factor (RF) for creep to limit the deformation and to ensure the integrity of the structure. The long-term strength value refers to service life of 50 or 100 years depending on the structure type. The creep reduction factor generally is the highest of all RF values. Thus, the creep behavior of geogrids has been intensively studied so that the appropriate RF can be incorporated into the long-term design of structural systems.

The creep property of geogrids varies with polymer type and service temperature with respect to the glass transition temperature (T_g), and melting temperature (T_m) of the polymer. Ideally, the creep behavior of geogrids should be evaluated according to ASTM D 5262, which requires a minimum of 10,000 hours (~ 1.1 years) testing time at the laboratory ambient condition. The creep data is then extended to one log cycle (e.g. from 10,000 to 100,000 hrs) with limited confidence. However, the extrapolated value is still far from the required 50 to 100 years design life (Greenwood et al. 2000). Therefore, accelerated creep tests with elevated temperatures are commonly utilized to predict the creep behavior.

Based on the equivalence between time and temperature, the time-temperature superposition (TTS) principle has been widely applied as a laboratory acceleration creep test. The result of the TTS creep test yields a creep master curve with duration much longer than the individual creep tests that were performed at elevated temperatures (Nielsen 1974; Ferry 1980; Painter and Coleman 1997). For HDPE geogrid, Farrag and Shirazi (1997) and Farrag (1998) obtained the creep properties using TTS and the test data was found to have good agreement with those from the conventional creep tests. The Boltzmann superposition principle (BSP) is another accelerated creep test in which the total strain of the test specimen is equal to the sum of the strain of each independent event (Moore and Kline 1984).

Stepped Isothermal Method (SIM) has been introduced to evaluate the creep property of geogrids for more than ten years. SIM combines the principles of both TTS and BSP by subjecting a single specimen to a series of temperature steps under a constant load to generate a sequence of creep responses (Thronton et al. 1998 a, b; Greenwood and Voskamp 2000). The similar test procedure has also been used to assess the creep behavior of polymethyl-methacrylate (PMMA) by Sherby and Dorn (1958). The major difference of SIM in comparison to TTS is the accumulated strain in the test specimen. In SIM, the induced creep strain at each temperature step is not removed, but accumulated in the test specimen. Contrarily, a new specimen is used for each test temperature in TTS; thus, test specimens do not possess pre-strain.

The validity of SIM has been investigated by comparing its creep data with those obtained from the TTS tests on the PET geogrid. Thornton et al. (1998b) compared SIM and TTS on PET yarns and found good agreement between two tests. The temperature increments, dwell time (i.e., isothermal duration), and method to generate the master strain curve for PET geogrids used in their study have been incorporated into the ASTM D 6992. In contrast, the applicability of SIM on the HDPE geogrid has not been thoroughly evaluated and a comprehensive assessment is required. The HDPE geogrid is in the rubbery state at the test temperature range, thus the creep response is expected to be very different than those of the PET geogrid that is in the glassy state. Furthermore, the HDPE geogrid has a relatively low melting point comparing geogrids made from other types of polymers. Therefore, plastic deformation would dominate the creep behavior of the HDPE geogrid, particularly at the high test temperatures. The accumulated

strain that is introduced to the test specimen of SIM may have a significant effect on the overall creep behavior, leading to a different creep deformation than from the TTS test.

In this paper, the creep strain of PET and HDPE geogrids was evaluated according to the SIM test procedure described in ASTM D 6992. Based on the test results, the applicability of SIM was discussed for both geogrids. Furthermore, a new data analysis procedure to generate the creep master curve was presented. The resulting master curves from ASTM and the modified method were compared to that from TTS. The differences were identified and discussed.

TEST MATERIALS AND APPARATUS

The physical properties of the PET and HDPE geogrids used in this study are listed in Table 1. A pictorial view of the test apparatus is shown in Figure 1 including a tensile machine, an environmental chamber, and a computer. A tensile machine, Instron® 5583, operated by Merlin® software for load control and strain measurement was utilized to perform all of the tests. The deformation of specimen was determined by the cross head movement, which was then divided by the initial gauge length to obtain the strain value. The test temperature was controlled by the environmental chamber. The constant temperature was kept inside the chamber with ± 0.5°C. The temperature at the specimen surface was monitored by a separate thermocouple during the testing. A set of box-type grips was used to hold the geogrid test specimens. The test specimen having three parallel ribs was mounted to the grips and then the two outer ribs were cut prior to starting the test. This mounting method provided a uniform loading on the central single rib. Due to the limited height of the environmental chamber, the HDPE geogrid test specimen did not conform to the configuration defined in ASTM D 6992; there was no horizontal rib in the middle of the specimen. The test targeted only the rib portion of the geogrid.

Table 1. Selected physical properties of the HDPE and PET geogrids

Property	Test standard	HDPE	PET
Unit weight (g/m^2)	ASTM D 5261	826	1067.9±11.8
Aperture size (mm) MD XD	Direct measurement	 121±2 5 to 15 (oval)	 33.4±0.4 33.5±0.8
Density (kg/m^3)	ASTM D 792	949	1370
Melting Temperature (°C)	ASTM 3418	140	249
Glass Transition Temperature (°C)	-	-150 to -90 Depending on the density and orientation	70 to 90 Depending on the orientation

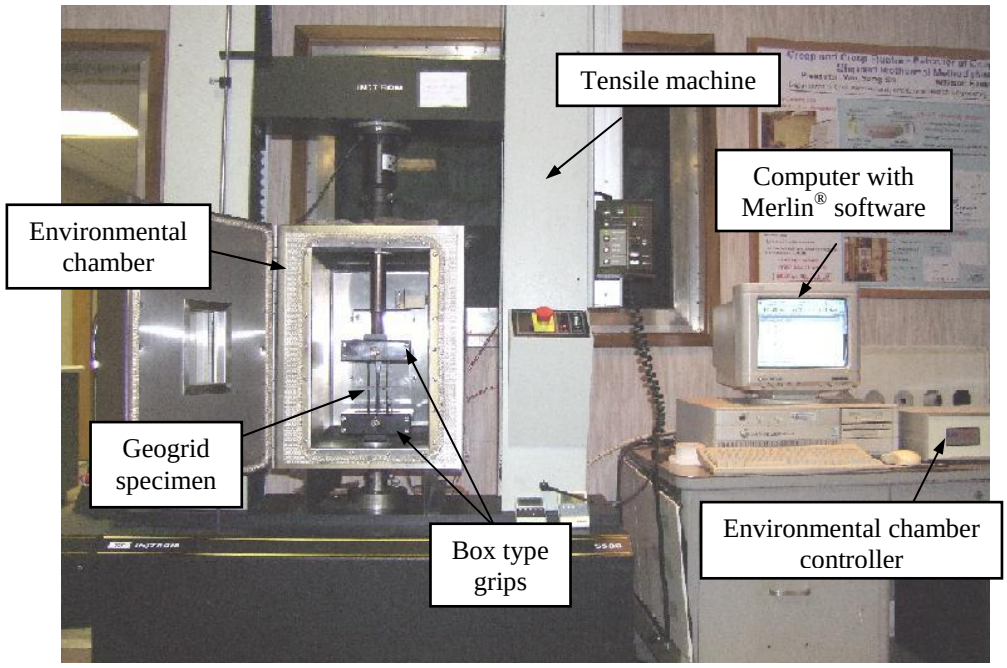

Figure 1. Pictorial view of the test apparatus

TENSILE STRENGTH OF SPECIMENS

The tensile tests of geogrids were conducted according to the test procedure described in ASTM D 6637. The loading was applied at a strain rate of 10% of the gauge length per minute. Five replicates were tested to obtain statistical significance. The load/deformation curves of the PET and HDPE test specimens are shown in Figure 2(a) and (b), respectively. The failures took place close to the middle of the rib in the PET geogrid specimen and in the upper portion of the HDPE geogrid. The HDPE geogrid exhibited a higher breaking elongation than the PET geogrid; while their breaking loads are relatively similar. The average ultimate tensile strengths (UTS) are 1.68 kN/strap (± 0.062) and 1.70 kN/rib (± 0.045) for the PET and HDPE geogrids, respectively. These UTS values were used to calculate applied loads for the accelerated creep tests.

The effect of test temperature on the tensile strength of geogrids was also evaluated by performing tensile tests at temperatures from 23 to 79°C. Figure 3 shows that the strength of both geogrids decreases as temperature increases. The tensile strength of the PET geogrid is less sensitive to temperature changes than the HDPE geogrid. This is because the testing temperature range is below the glass temperature and much lower than melting temperature of the PET geogrid. However, the testing temperature range is well above the glass temperature and relatively close to the melting temperature of the HDPE geogrid.

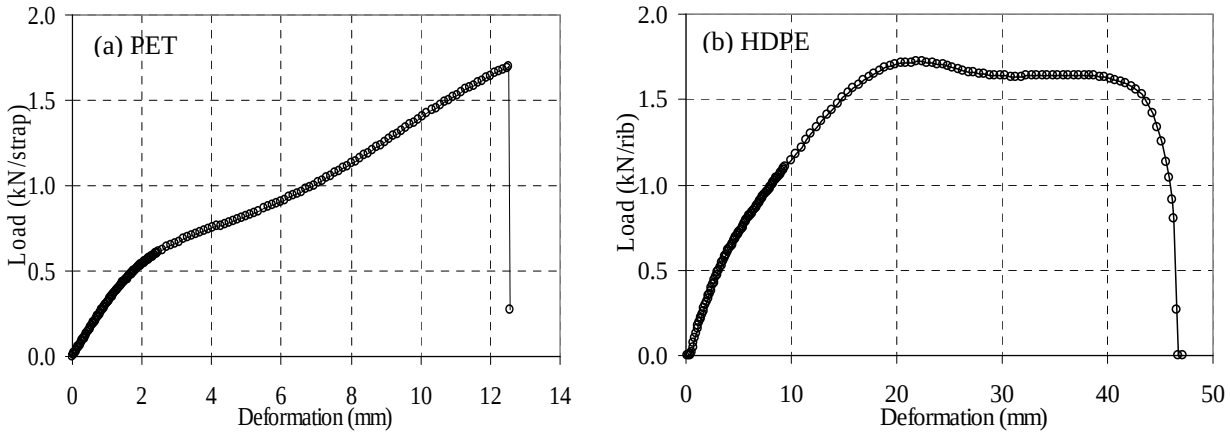

Figure 2. Load/deformation curves for (a) PET and (b) HDPE geogrids

TEST METHOD

The SIM tests were performed according to ASTM D 6992. The test specimen was brought to equilibrium at 23 ± 2°C overnight. Prior to starting the test, a pre-stress of one percent of the tensile strength was applied to the specimen. The test was started by loading the specimen at a strain rate of 10% of the gauge length per minute to reach the desired applied load. The applied loads (or stress) were 30% and 50% of UTS for the PET geogrid and 20% and 40% of UTS for the HDPE geogrid. The PET test specimens were exposed to five temperature steps from 23 to 79°C with increments of 14°C. For HDPE geogrid specimens, eight or nine temperature steps were employed from 23 to 72 (or 79)°C with increments of 7°C. The use of different temperature increments for the two types of geogrids is due to the temperature influence on their tensile properties, as shown in Figure 3. At the initial portion of each test temperature, the data was collected for every 10 seconds up to 150 seconds. After that, the data was recorded every 60 seconds. The isothermal duration (i.e., dwell time) at each temperature was 10^4 seconds (~ 2.7 hours). Example of the SIM testing data of PET and HDPE geogrids is presented in Figure 4(a) and (b), respectively. The creep strain increases with temperature and time.

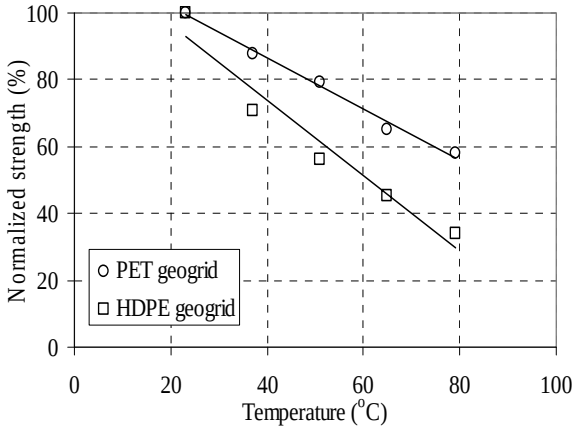

Figure 3. Ultimate tensile strengths at elevated temperatures

TTS tests were also performed on the two types of geogrids and the procedures were based on that described in Farrag and Shirazi (1997). The test specimen was brought to equilibrium at the desired test temperature for 3 hours. Prior to starting tests, a pre-stress of one percent of the ultimate tensile strength obtained at 23°C was applied. The test was started by loading the specimen at a strain rate of 10% of the gauge length per minute until the target load level was reached. Each temperature condition of 23, 37, 51, 65, and 79°C for the PET geogrid and of 23, 30, 37, 44, 51, 58, 65, and 72°C for the HDPE geogrid were kept for 10^4 seconds (~ 2.7 hours). A new test specimen was used for each test temperature. The frequency of data collection is the same as that of the SIM test. The creep master curve is created by joining the individual creep curve at each elevated temperature through horizontally shifting along the log-time axis.

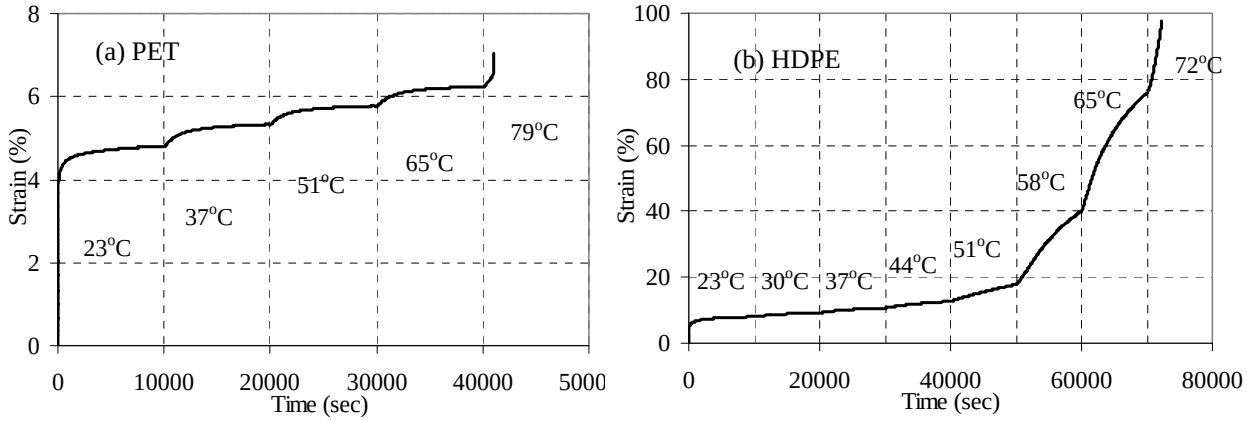

Figure 4. Testing data of SIM for (a) PET and (b) HDPE geogrids

DATA ANALYSIS AND TEST RESULTS

Creep Master Curve According to ASTM Procedures

Figure 5 shows the analytical procedure to generate the creep master curve from the SIM data described in ASTM D 6992. Figure 5(a) shows the testing data obtained from a general SIM test. According to Thornton et al. (1998a), the virtual times, t_n' , should be used to rescale the creep curve at each elevated temperature since creep at the higher temperature have occurred at an earlier time than the starting time at each temperature (i.e., segment onset time), t_n, if a new specimen was used at each elevated temperature. The t_n' is determined by iteratively varying a candidate t_n' until a close match between the initial slopes of the strain curves and the end slope of the previous strain curve in the plot of creep strain vs. log time (Allen 2005). With SIM data, t_n' at each elevated temperature are determined as indicated in Figure 5(b). The creep curves at each elevated temperature can be then rescaled by subtracting t_n' from the data in each of temperature steps (S_n), as shown in Figure 5(c). In this method, there is no overlapping between two consecutive strain curves. The total creep strain equals to the sum of the individual strain, assuming that BSP is applicable to the test data. The rescaled creep curves in Figure 5(c) can then be shifted horizontally to achieve the creep master curve, as shown in Figure 5(d).

Based on the ASTM procedure, the creep master curves of PET and HDPE geogrids were created, as shown in Figure 6(a) and (b), respectively. The t_n and t_n' at each temperature step are listed for both geogrids in Table 2. The HDPE geogrid exhibits a much larger time difference (i.e., $t_n - t_n$') than the PET geogrid. This is because the HDPE geogrid is more sensitive to temperature changes than PET at the test temperature range. The HDPE geogrid also has a higher thermal expansion than the PET geogrid, leading to a greater influence in the initial portion of each creep curve. In the tensile creep test, the thermally induced strain acted in the same direction as the mechanically induced creep strain; thus, they cannot be visually separated from the raw test data, as shown in Figure 4. Due to the uncertainty of the initial portion of individual creep curve, that portion of the curve should not be included in the data analysis.

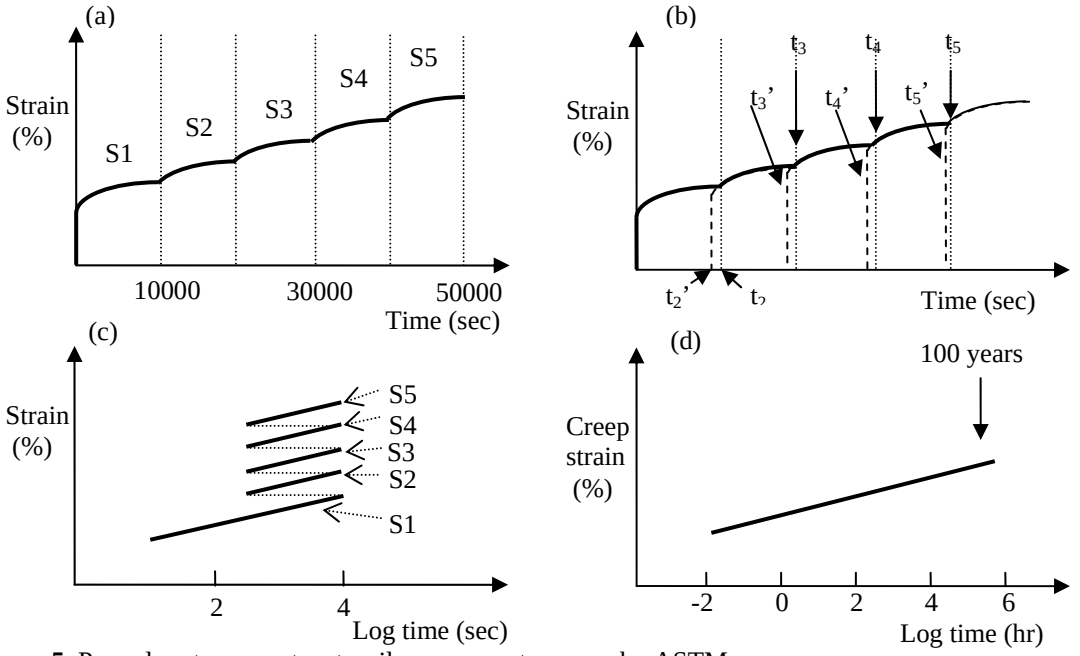

Figure 5. Procedure to generate a tensile creep master curve by ASTM

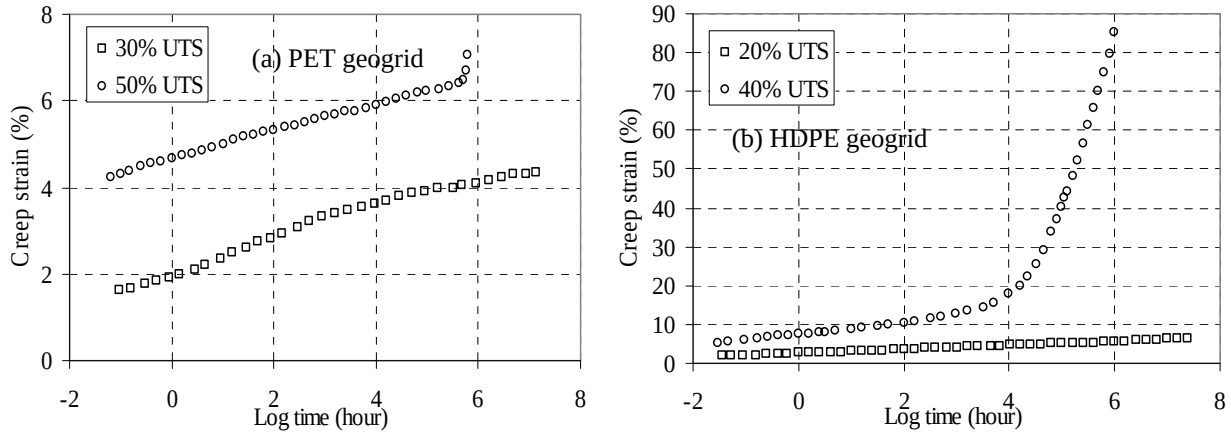

Figure 6. Creep master curves of (a) PET and (b) HDPE geogrids by ASTM

Table 2. Real and virtual starting times on SIM

step	PET geogrid						HDPE geogrid					
	t_n (sec) *		t_n' (sec) †		t_n-t_n' (sec)		t_n (sec)		t_n' (sec)		t_n-t_n' (sec)	
	30%	50%	30%	50%	30%	50%	20%	40%	20%	40%	20%	40%
1‡	0	0	0	0	0	0	0	0	0	0	0	0
2	10115	10080	9948	9850	167	230	10094	10128	9570	8416	524	1712
3	20075	20100	19850	19850	225	250	20114	20148	18750	18401	1364	1747
4	30095	30120	29976	29850	119	270	30074	30168	28610	28438	1464	1730
5	40115	40080	40000	39850	115	230	40094	40128	38500	38611	1594	1517
6	N/A	N/A	N/A	N/A	N/A	N/A	50114	50088	49000	48910	1114	1178
7	N/A	N/A	N/A	N/A	N/A	N/A	60074	60108	59020	58229	1054	1879
8	N/A	N/A	N/A	N/A	N/A	N/A	70092	70068	69020	66654	1072	3414
9	N/A	N/A	N/A	N/A	N/A	N/A	80112	N/A	79150	N/A	962	N/A

*t_n = real starting time
†t_n' = virtual starting time;
‡Step 1 (i.e., reference temperature): 23°C
§Temperature increments: 14°C for the PET geogrid and 7°C for the HDPE geogrid

Creep Master Curve According to Modified Procedures

The new procedure to analyze the SIM creep data is to eliminate the initial non-equilibrium stage caused by thermal expansion and temperature change. The new procedure is illustrated in Fig. 8, and is called the modified SIM (MSIM) in this paper. Figure 7(a) shows a illustration of testing data, which is the same as Figure 5(a). The strain curves at elevated temperature steps are rescaled to the reference temperature (e.g., 23°C) along the log scale of time axis by subtracting the starting time of each temperature step (i.e., $t_{1, 2, 3, etc}$), as shown in Figure 7(b). The virtual time, t_n', is not involved in this analysis. Figure 7(c) shows the rescaled creep curves in which the initial non-equilibrium portion of the curve that exhibits a different slope is discarded. Vertical shifts are required to accommodate the gaps created by the removal of initial portion of the curve. On the molecular scale, the vertical shifting can be explained by the influence of changes in the crystalline structure of polyethylene on its relaxation modulus with temperature (Popelar et al. 1991; Tobolsky 1960). Figure 7(d) shows the creep master curve after using both horizontal and vertical shifting. Using the MSIM procedure, creep master curves of PET and HDPE geogrids are shown in Figure 8(a) and (b), respectively.

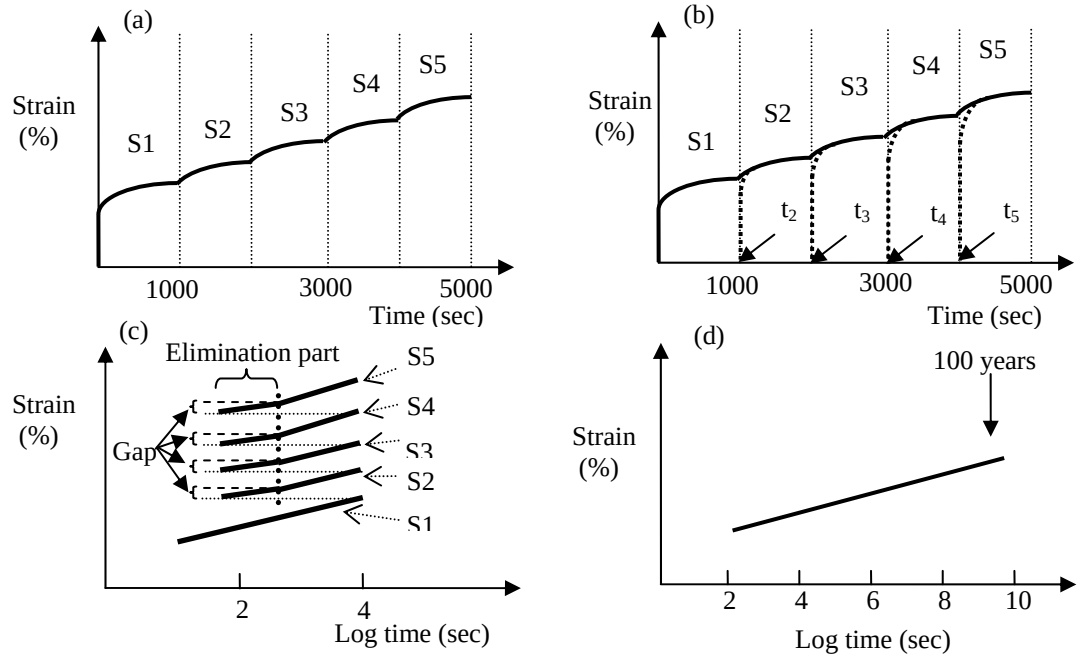

Figure 7. Modified procedure to generate a tensile creep master curve

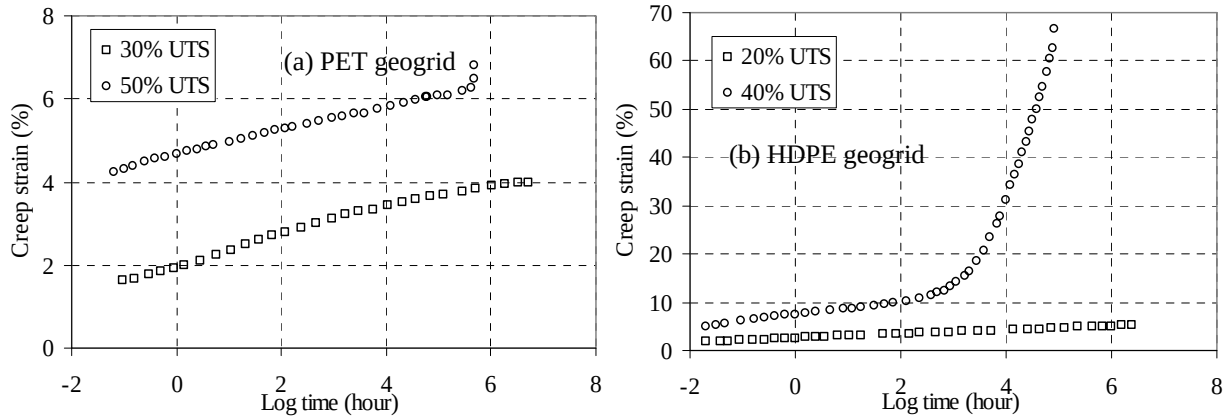

Figure 8. Creep master curves of (a) PET and (b) HDPE geogrids by modified method

DISCUSSION

Comparison among SIM, MSIM, and TTS

Figure 9 presents the creep master curves obtained from SIM, MSIM, and TTS. For the PET geogrid, the three master curves under 30% and 50% UTS exhibit a linear relationship between the creep strain and log time, as shown in Figure 9(a). The three curves were matched each other. The result confirms the applicability of SIM in predicting the creep behavior of PET geogrid. For the HDPE geogrid, the three master curves at 20% UTS and 40% UTS up to 10% creep strain exhibit a linear relationship between creep strain versus log time, and they are very similar to each other, as shown in Figure 9(b) and (c). However, as the creep strain exceeds 10% entering the non-linear portion of the master curve, a deviation is observed among SIM, MSIM and TTS; the MSIM curve is closer to the TTS curve.

This significant difference is particularly because the combination of high thermal expansion and plastic deformation of the HDPE geogrid led to a large non-equilibrium stage at 72°C, as reflected by the significantly high *t*-t_n' value in Table 2. By incorporating the non-equilibrium stage into the SIM curve could lead to greater uncertainty in the prediction.

Creep Mechanism

Besides comparing the creep master curves, the creep mechanism of the accelerated creep tests is investigated using the activation energy, which can be defined as an energy barrier that must be overcome for the occurrence of molecular motions and is governed by stress and temperature (Findley 1960; Goertzen and Kessler 2006). The activation energy can be obtained by plotting the horizontal shift factor (a_T) against reciprocal test temperatures according to Arrhenius equation, as expressed in Eq 1:

$$\log a_T = \frac{Q}{2.303R}\left(\frac{1}{T} - \frac{1}{T_{ref}}\right) \qquad \text{(Eq. 1)}$$

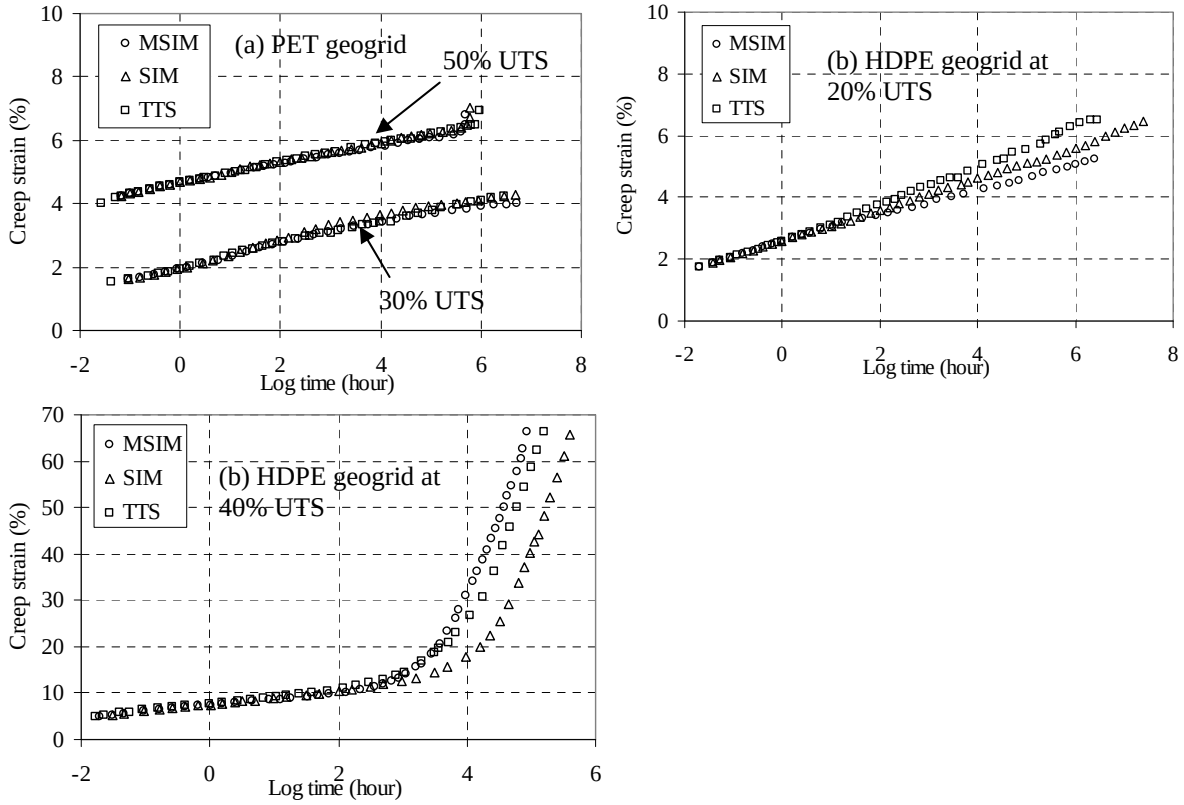

Figure 9. Comparison between two SIM curves and TTS curve for the (a) PET geogrid at 20% and 50% UTS, (b) HDPE geogrid at 20% UTS, and (c) HDPE geogrid at 40% UTS

Where Q is activation energy in J/mol, R is gas constant (8.314) in J/mol·K, T is absolute temperature in K, T_{ref} is reference temperature in K. Table 3 shows the activation energy values of the PET and HDPE geogrids based on SIM, MSIM, and TTS with a dwell time of 10^4 seconds. Overall, lower activation energy values were observed at higher applied loads for both geogrids, particularly for the HDPE geogrid. Sherby and Dorn (1958) accounted for this behavior as stress decreases the thermal energy requiring for polymer flow.

Under the same applied load, the three activation energy values of the PET geogrid are relatively close. Also, these values are similar to those presented in published literature. Lim et al. (2003) acquired the activation energy of PET ranging from 233.9 to 269.6 kJ/mol. They indicated that the changing of the activation energy was caused by the crystallinity of PET; the energy increases with the crystallinity. Foot et al. (1987) also reported activation energy of 190 kJ/mol for the isotropic amorphous PET.

For the HDPE geogrid, there is noticeable difference in the activation energies among SIM, MSIM, and TTS at both applied loads; SIM shows the highest values than those from MSIM and TTS. In the published literatures, a wide range of activation energies was reported for HDPE materials. Govaert et al. (1993) found an activation energy value of 118 kJ/mol for PE fibers. Cembrola and Stein (1980) obtained energy values of 85 ± 30 kJ/mol by studying the stress relaxation of an oriented HDPE; similar activation energies were also obtained by Farrag and Shirazi (1997) and Farrag (1998) on HDPE geogrids using TTS. Thornton (1970) performed creep tests on HDPE at elevated

temperatures and obtained an activation energy of 115.8 kJ/mol, which is comparable to the activation energy of 125.6 kJ/mol obtained by McCrum and Morris (1964) with the same material. A direct comparison between the resulted values and published ones is difficult since most papers did not present the applied load in terms of percentage of UTS. Nevertheless, the activation energy from the MSIM at 40% UTS is closer to the published values.

Table 3. Activation energy for PET and HDPE geogrids based on SIM, MSIM, and TTS

Applied Load % UTS	PET Geogrid			HDPE Geogrid		
	SIM	MSIM	TTS	SIM	MSIM	TTS
20	-	-	-	268.0	236.3	234.4
30	258.3	241.7	220.2	-	-	-
40	-	-	-	166.5	115.2	142.9
50	209.0	212.5	205.4	-	-	-

CONCLUSION

A new procedure, MSIM, was suggested to analyze the SIM testing data to generate the creep master curve since the current procedure described by ASTM D 6992 did not consider the non-equilibrium stage at the beginning of each elevated temperature step. The MSIM procedure utilized the segment onset time, t_n, instead of virtual time, t_n', in the rescaling of individual creep curve. For the PET geogrid, the creep master curves and activation energy values are very similar regardless the test methods and data analysis procedures. However, for the HDPE geogrid, SIM would underestimate the creep deformation in comparison to TTS and MSIM at the creep strain exceeding 10% when the creep strain versus log-time curve becomes non-linear. Furthermore, higher activation energies were obtained from SIM than those from MSIM and TTS.

This study verifies that SIM is a sophisticated acceleration method to predict the creep deformation of geosynthetic materials that possess a linear creep strain versus log-time behavior. However, MSIM is a more appropriate data analysis procedure for predicting non-linear creep behavior or materials with unknown creep behavior.

Acknowledgement: The research project is sponsored by the Center for Polymer Reinforced Structures (CPReS) of Geosynthetic Institute (GSI).

REFERENCES

Allen, S.R. 2005. The use of an accelerated test procedure to determine the creep reduction factors of a geosynthetic drain. Geotechnical special publication, Geo-Frontier 2005, 3297-3309.

Carroll, R.G., Chouery-Curtis, V. 1991. Geogrid reinforcement in landfill closures. Geotextiles and Geomembranes, 10(5-6), 471-486.

Cembrola, R.J., Stein, R.S. 1980. Crystal Orientation Relaxation Studies of Polyethylene. Journal of polymer science: Polymer physics edition, 18, 1065-1085.

Fannin, R.J. 2001. Long-term variations of force and strain in a steep geogrid-reinforced soil slope. Geosynthetics international, 8(1), 81-96.

Farrag, K. 1998. Development of an accelerated creep testing procedure for geosynthetics- part II: analysis, Geotechnical testing journal, 21(1), 38-44.

Farrag, K. Shirazi, H. 1997. Development of an accelerated creep testing procedure for geosynthetics-part I: testing. Geotechnical testing journal, 20(4), 414-422.

Ferry, J.D., 1980, Viscoelastic properties of polymers, 3rd ed., John Wiley and Sons, NY. USA.

Findley, W.N. 1960. Mechanism and mechanics of creep of plastics. Society of plastics engineers (SPE) journal, 16(1), 57-65.

Foot, J.S., Truss, R.W, Ward, I.M., Duckett, R.A. 1987. Yield behaviour of amorphous polyethylene terephthalate: An activated rate theory approach, Journal of materials science, 4, 1437-1442.

Greenwood, J.H., Voskamp, W. 2000. Predicting the long-term strength of a geogrid using the stepped isothermal method. 2nd European geosynthetics conference (EuroGeo2), Italy, 329-331.

Greenwood, J.H., Kempton, G.T., Watts, G.R.A., Bush, D.I. 2000. Twelve year creep tests on geosynthetic reinforcements. 2nd European geosynthetics conference (EuroGeo2), Italy, 333-336.

Goertzen, W.K., Kessler, M.R. 2006. Creep behavior of carbon fiber/epoxy matrix composites. Materials science and engineering A, 421, 217-225.

Govaert, L.E., Bastiaansen, C.W.M., Leblans, P.J.R. 1993. Stress-strain Analysis of Oriented Polyethylene. Polymer, 34(3), 534-540.

Koerner, R. M., 2005, Designing with Geosynthetics, 5th ed., Prentice Hall, Englewood Cliffs, NJ. USA. pp796.

Lim, J.Y., Donahue, H.J., Kim, S.Y. 2003. Strain rate, temperature, and microstructure-dependent yield stress of poly(ethylene terephthalate). Macromolecular chemistry and physics, 204(4), 653-660.

McCrum, N.G., Morris, E.L. 1964. On measurement of activation energies for creep and stress relaxation. Royal Society – Proceedings Series A, 281(1385), 258-273.

Moore, G.R., Kline, D.E. 1984. Properties and processing of polymers for engineers. Prentice-Hall Inc., Englewood Cliffs, NJ, USA. pp209.

Nielsen, L.E. 1974. Mechanical properties of polymers and composites, Vol. 1, 2, Marcel Dekker Inc., NY. USA.

Painter, P.C., Coleman. M. M. 1997. Fundamentals of polymer science, 2nd Ed., CRC press, Boca Raton, FL. USA.

Popelar, C.H., Kenner, V.H., Wooster, J.P. 1991. An accelerated Method for establishing the long term performance of polyethylene gas pipe materials. Polymer engineering and science, 31(24), 1693-1700.

Sherby, O.D., Dorn, J.E. 1958. Anelastic Creep of Polymethyl Methacrylate. Journal of mechanics and physics of solids, 6, 145-162.

Thornton, A.W. 1970. Creep of polyethylene above room temperature. Journal of applied physics, 41(11), 4347-4350.

Thornton, J.S., Paulson, J.N., Sandri, D. 1998. Conventional and stepped isothermal methods for characterizing long term creep strength of polyester geogrids. 6th international conference on geosynthetics, Atlanta, GA, USA. 691-698.

Thornton, J.S., Allen, S.R., Thomas, R.W., Sandri, D. 1998. The stepped isothermal method for time-temperature superposition and its application to creep data on polyester yarn. 6th international conference on geosynthetics, Atlanta, GA, USA. 699-706.

Tobolsky, A. V., 1960, Properties and structure of polymers, John Wiley and Sons, NY. USA.